DESIGN OF LOW-DRAG AUTONOMOUS UNDERWATER VEHICLES AND FLOW CONTROL

(DOI No: 10.3940/rina.ijme.2016.a1.338)

E Amromin, Mechmath LLC, USA

SUMMARY

Design of autonomous underwater vehicles (AUV) met the opposite challenges. Their achievable route can be enhanced with drag reduction due to an increase of AUV slenderness. However, blunt short AUV have others operational advantages. The possibility to design low-drag bodies for Reynolds numbers employed by contemporary AUV ($2\times10^6<Re<10^7$) is based on a combination of known facts. First, blunt bodies experience a drag crisis associated with laminar-turbulent transition in their boundary layers and some boundary layer suction additionally reduces their drag. Second, the transition can be delayed till much higher Re for bodies without adverse pressure gradients over their forward and medium parts. Suction on sterns of such bodies allows for the very substantial drag reduction. Several body shapes with distributed suction with extremely low slenderness ($L/B<1.5$) are presented. Their drag coefficients are between 0.007 and 0.02, whereas for ellipsoid of the same slenderness it exceeds 0.08.

NOMENCLATURE

B	Beam (m)
C_D	Drag coefficient
Cp	Pressure coefficient
L	Length (m)
Q	Suction intensity (m^4/s^2)
Re	Reynolds number
S_W	Wetted surface area (m^2)
T	Draft (m)
U	Longitudinal velocity component within boundary layers (m/s)
U	Speed of AUV (m/s)
U_δ	Velocity out of the boundary layer (m/s)
Um	Maximum AUV speed (knots)
W	Velocity of secondary flow within 3D boundary layer (m/s)
ρ	Density of fluid (kg m^{-3})
δ^*	Displacement thickness of boundary layer (m)

1. INTRODUCTION

Currently, there are many dozens of various autonomous underwater vehicles. Nevertheless, the majority of them belong to two classes.

One class is composed from axisymmetric bodies. Shapes of these bodies were typically copied from the torpedo shapes. Such a copying is a quite strange decision because AUV and torpedo motions are usually very different. In particular, AUV should not run at speeds over 40 knots (f. e., Um of the REMUS 600 is 4 knots, though it is one of the fastest AUV), whereas torpedoes are not assigned to chaise their targets during 10 hours or longer. So, a torpedo shape cannot be hydrodynamically optimal for AUV.

Shapes of another class of AUV remind rather the bathyscaph shapes. They have low slenderness (ratios L/B) with ratios B/T close to 1.0. For example, SENTRY (designed by WOI) has L/B=1.32 and B/T=1.22, ODYSSEY IV (designed by MIT) has L/B=1.73 and B/T=1.15. Enhancement of hydrodynamic performances is a greater challenge for this class. Because AUV are mainly either axisymmetric bodies or bodies with a slight deviation from the axial symmetry, their dependency of drag on slenderness can be evaluated with Figure.1 providing results for ellipsoids. There one can see the very high drag coefficients for L/B ratios corresponding to SENTRY and ODYSSEY IV.

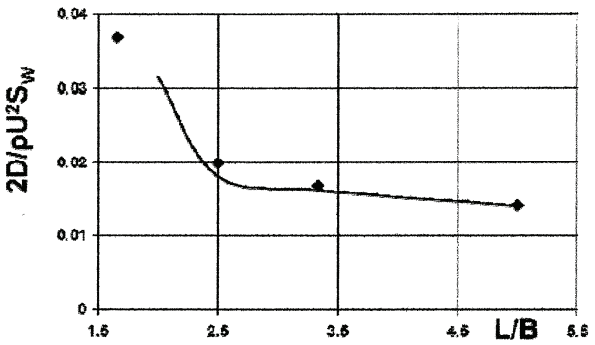

Figure 1: Ellipsoid drag coefficients versus its slenderness; rhombus – measurements; line – computations

The AUV friction coefficients at their Reynolds numbers are around 0.003. So, the major part of drag described by Figure.1 is their form resistance.

A substantial drag reduction is necessary to enhance the operational capabilities of the second class AUV. Seeking the drag minima of blunt bodies, one may find data in the Hoerner famous monograph [1]. As noted there, for spheres and other blunt bodies, the drag minima exists in the range of Reynolds number corresponding to the appearance of laminar-turbulent transition in the body boundary layers (please keep in mind that the drag coefficient C_D in [1] and below in this paper is normalized by the body cross-section that is smaller than S_w and because of this the coefficients are at least fourfold greater than presented in Figure.1). One

can see in Figure.2 that these drag minima (at Re=7×10^5 for the body related to this figure) is associated with displacement of the boundary layer separation to the stern and this results in an increase of base pressure.

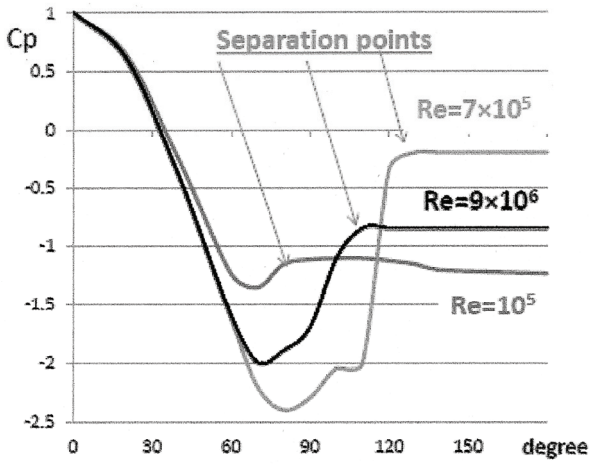

Figure 2: Effect of Reynolds number on pressure distribution along meridian section of a blunt body

It is also described in [1] that these minima can be made even substantially lower by means of a boundary layer suction applied in the areas of the adverse pressure gradients. This occurs because such suction displaces the boundary layer separation downstream to the stern. Then the drag of the bodies drops because the area covered by a separation zone becomes smaller and the base pressure inside it becomes higher.

However, data presented in [1] relate to Re<10^6 only, whereas Re of AUV varies from 3×10^6 for SENTRY to 7×10^6 for REMUS600 and the challenge is to get transition-related drag minima at Re→10^7. Is transition possible at such Reynolds numbers?

As proven by the water tunnel experiments [2], under a favourable pressure gradient the boundary may be laminar at least up to Re=4×10^6. So, the first issue is to design bodies with the pressure gradient favourable for such late transition, and this is a passive flow control.

Further, as already stated, the short bodies have high drag coefficients due to extensive boundary layer separation zones on their sterns. The boundary layer separation conditions can be characterized by the product of the pressure gradient and the boundary layer displacement thickness. Separation of turbulent boundary layer occurs when the left-hand side of the inequity

$$\frac{\delta^*}{1-Cp}\frac{\partial Cp}{\partial s} > \chi \qquad (1)$$

exceeds some empirical constant χ. The constant χ for this semi-empirical criterion can be taken from the paper [3]. The derivative of Cp unavoidably will be high at least at a part of the body stern and the only path to reduce the left-hand side of the expression (1) in this part of the stern is to reduce δ^* there. So, the second issue is the local reduction of the boundary layer thickness displacement and it is more likely to achieve this reduction with an active flow control.

2. DESIGN CONCEPT

The objective of the considered inverse hydrodynamic problem is to displace zones of high adverse pressure gradients as far as possible downstream and reduce the boundary layer thickness within these zones. As was recently proven [4], achievement of this double objective is possible with a special combination of passive and active flow control. This combination for the axisymmetric body is illustrated by Figure.3.

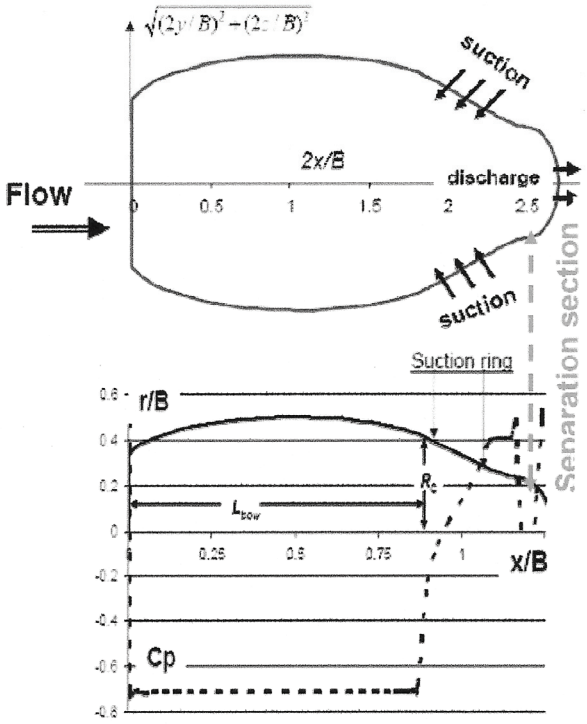

Figure 3: Section of designed AUV hull with L/B=1.35 (top) and pressure coefficient along it (bottom)

An innovative AUV design concept suggested in this paper includes:

1. Displacement of the area of high adverse pressure gradient to the stern by variation of the vehicle hull shape (this is the passive flow control). As shown in Figure.3, such a passive control displaces the zone of an adverse pressure gradient far downstream to the stern. This displacement delays both the boundary layer transition and its separation. The simplest way to displace the adverse pressure gradient zone is to design a hull with a large constant pressure central part.
2. Application of a suction to the area of high pressure gradient downstream of the constant

pressure zone with the aim to prevent boundary layer separation there (this is an active flow control).

The results presented below are numerical results. Therefore, even avoiding descriptions of the employed numerical method and readdressing to [4] for them, author provides some examples of their validation. There is no necessity in validation for the method to design constant pressure forms because the corresponding mathematical problem coincides with the problems on cavitation in ideal fluid and the proven numerical technique for them does not include any empirics. However, for computations of boundary layers, validations with experimental data are necessary.

First of all, employing integral methods for boundary layers, one has to compare computed velocity profiles with data for the same body in the same *Re*. Such validation example is shown in Figure.4 for the axisymmetric ellipsoid of *B/L*=6 with a conical trailing edge frequently named as "Patel Body". Computations for Figure.4 were carried out with use of the velocity profile $u(y)=f(\eta)+[U_\delta - f(\delta)]\,\eta^2[3-2\eta]$, where $\eta=y/\delta$, y is the boundary layer lateral coordinate, δ is the layer thickness, $f = 2.5v^*\left(\ln\left|yv^*/\nu\right|+5.2\right)$, v^* is friction velocity.

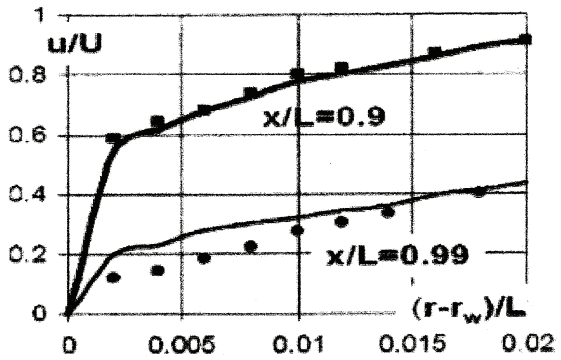

Figure 4: Comparison of computed and measured [5] velocity profiles around PB at *Re*=7×10^6

The transition zone location must be satisfactory predicted in this problem. Regardless to the recent achievements of computational fluid dynamics (aimed, by the way, mainly on studies of fully turbulent flows), the very old empirical Michel criterion [6]

$$\frac{U_\delta \delta^{**}}{1.174\nu} = \left(\frac{U_\delta s}{\nu}\right)^{0.46} + 22400\left(\frac{\nu}{U_\delta s}\right)^{0.54} \qquad (2)$$

remains to be the most reliable for transition determination (and was used in [2], [4], etc.). Here δ^{**} is the boundary layer momentum thickness, s is arc abscissa counted along streamline on the body surface. Such a line is an oversimplification of the real transition zone, but, as shown in Figure.5 for the "Patel Body" tested by another team [7], its location is satisfactory found with the criterion (2) and this criterion is applicable even to 3D flows. The laminar boundary layer upstream of this line can be computed with many integral methods well-described in various monographs.

Finally, the accuracy of drag calculation for short bodies directly depends on the accuracy of base pressure computations. Let us assume that the separation zone behind bodies is a constant pressure zone. As seen in Figure.1, this assumption worked well for ellipsoids. It was also validated for a self-driven body with a blunt transom: according to the experiment [8], an error in its drag computation with such assumption was under 5%.

There is also a far wake downstream of this zone. So, the whole flow was broken into five parts: the outer inviscid flow, the laminar boundary layer, the turbulent boundary layer (with suction in some its part), the stern separation zone and the far viscous wake.

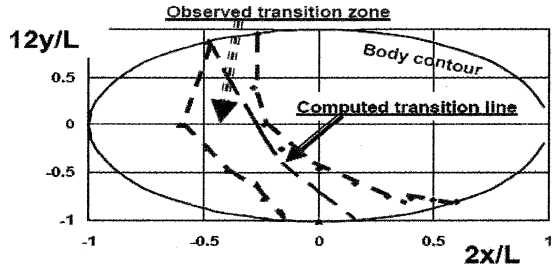

Figure 5: Computed and measured [7] transition zone on PB at *Re*=7×10^6 and 10 degree angle of attack

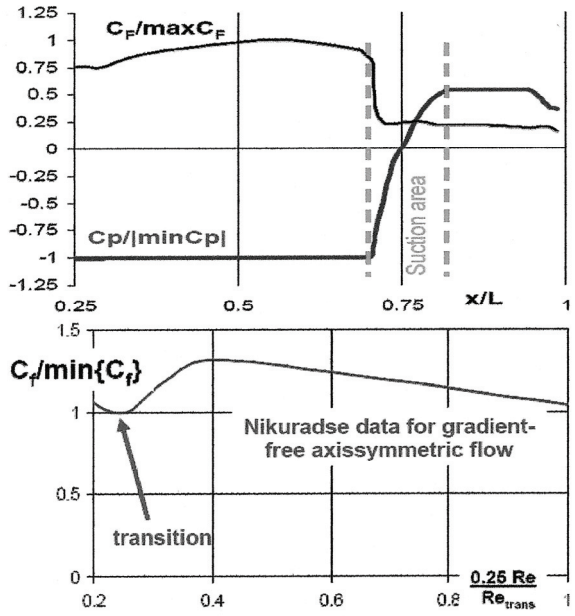

Figure 6: Computed friction and pressure coefficients for the designed body with boundary layer suction at Re=4×10^6 (top) and the experimental dependency for friction downstream of transition zone in flows without pressure gradient (bottom)

The physics of the described combination of passive and active flow control is illustrated here in more detail for a designed body with L/B=2.2. As shown in Figure.6, on the body central part downstream of the transition zone the wall friction experiences a slight variation, whereas the pressure remains constant there. This friction variation is very similar to the well-known measured (by Nikuradze, in 1930s) dependencies in axissymmetric flows without pressure gradient in post-transition conditions. The unavoidable zone of a sharp increase of the pressure coefficient Cp begins from the section x=0.7L of this body. Correspondingly, a sharp drop of friction coefficient takes place there, but the boundary layer suction makes it possible to keep δ^* below the limit prescribed by the above-mentioned separation criterion (1).

As shown in Figure.7, for the flow without suction (at Q=0) the boundary layer separation starts just downstream of the constant pressure zone. Further, there is a minimum value Q=Q_{min} allowing for a small displacement of the separation zone with a small gain in the body drag. The following threefold increase of Q makes it possible to displace this zone practically to the body trailing edge. The friction distribution in Figure.6 corresponds to this Q.

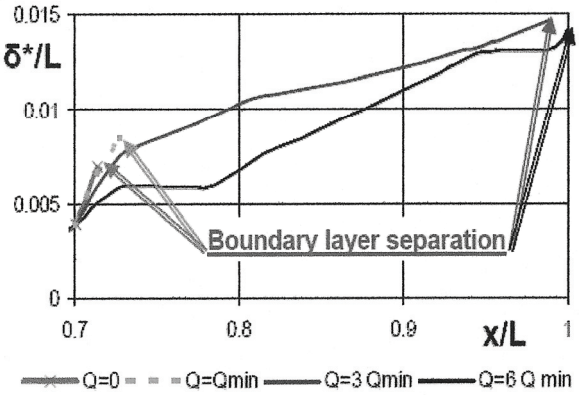

Figure 7: Suction effect on the boundary layer displacement thickness at Re=4×10^6

The following twofold increase of Q does not provide a significant additional drag reduction, though some reduction of the cross-section area of separation zone then occurs. The subsequent increase of Q can give even a negative effect due to both an additional energy spending for an increase of Q and the appearance of inverse flows downstream of the suction area. The effect of Q on thickness displacement of the boundary layer is clearly seen in Figure.7.

Further, design of the second constant pressure zone downstream of the suction ring is included in the described design concept. This constant pressure zone allows for the subsequent displacement of the high adverse pressure gradient zone to the stern. As a result, the zone of viscous separation in the body stern covers smaller stern area and the base pressure will be higher. As already noted, both effects reduce the body drag. Also, the substantial dependency of the achieved drag minima on stern form is seen in Figure.8. Examples of the very short hulls presented there manifest the possibility to significantly reduce drag. By the way, the hulls presented in Figures.3 and 8 have about exactly the SENTRY slenderness.

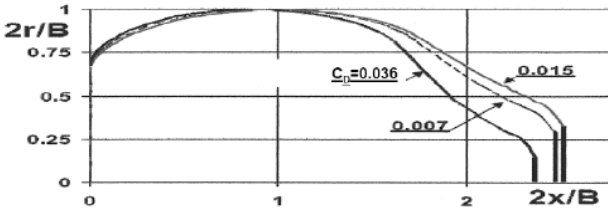

Figure 8: Meridian sections of axisymmetric hulls with various sterns designed for Re=10^7

3. EFFECT OF REYNOLDS NUMBER

Because the suggested drag reduction technique is associated with the control of laminar-turbulent transition, an effectiveness of this technology certainly should depend on Reynolds number. The presented data on the Reynolds number effect are numerical results, but, these results are in the qualitative accordance with known experimental data. As illustrated by Figure.9, the boundary layer suction can sharply reduce the total drag. The minimum of the drag coefficient at Re~3×10^6 is smaller than 0.01.

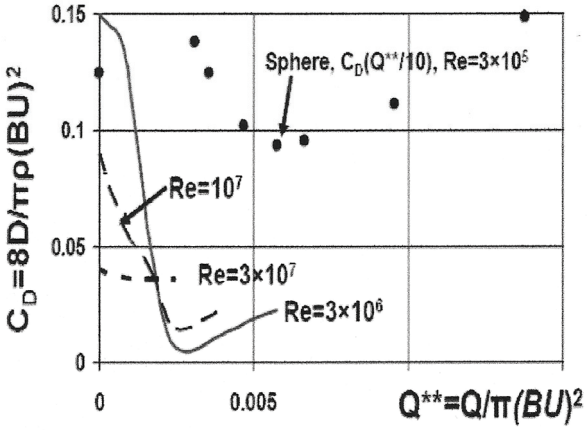

Figure 9: Comparison of computational results for the designed axisymmetric body with L/B=1.3 and experimental data [1] for suction effect on sphere drag. Here Re is calculated using B

On the other hand, the excessive suction has an inverse effect provoking a reverse flow on the body surface. Correspondingly, the sharp dependencies of the body drag on the suction intensity are also seen in Figure.9. The suction is effective only at moderate Reynolds numbers and the suction advantage at Re=3×10^7 became insignificant (let us note that for this body the ratio L/B is quite close to 1.0 and Re based on L will be

insignificantly greater than *Re* based on *B*). Fortunately, the found range of suction effectiveness coincides with the range of AUV Reynolds numbers.

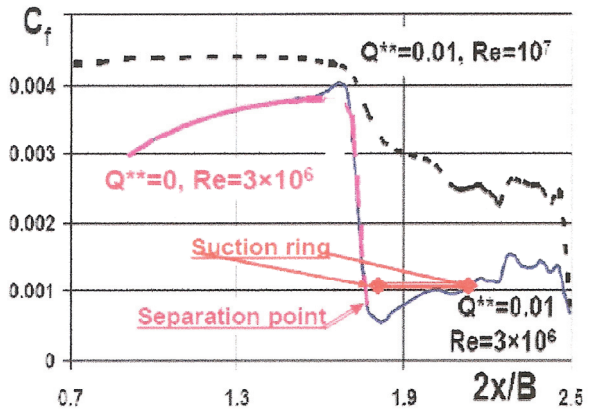

Figure 10: Effect of suction on friction and location of boundary layer separation for a designed body. Here $Q^{**}=Q/[\pi(BU)^2]$, *Re* is calculated using *B*

The physics behind the combined effect of *Re* and suction intensity is illustrated by Figure.10. Without suction (for $Q^{**}=0$) the boundary layer separation occurs at $x=0.9B$ (at $x\approx0.7L$), but there is no separation with the applied suction for $x/L<0.9$. The wall friction sharply drops at separation zones, but the friction is also low in the transition zone. The suction effect is the highest at $Re=3\times10^6$, where a synergy with drag reduction due to laminar-turbulent transition takes place.

Let us, however, point out that a 90% drag reduction will not result in the tenfold increase of the AUV mission duration because a fraction of the available energy will be consumed by its equipment. With 25% of battery power spent for AUV equipment, such drag reduction gives only 140% increase of this duration and the necessity to install a suction system may reduce it even with a smaller engine requiring the smaller power.

4. THREE-DIMENSIONAL EFFECTS

The suggested combination of the passive flow control and the active flow control will work for both axisymmetric and 3D flows. Such tree-dimensional hull shapes also can have small length to beam ratios. Besides, as shown in examples of 3D constant pressure shapes provided in [4], it is possible keep the large flat surface areas at their bows (that are very convenient for many kinds of equipment), but there are certain geometrical restrains on such 3D shapes. In particular, the attempts to design a constant pressure area covering a major part of the body surface with the substantial asymmetry of cross-sections (with the dimension ratios $B/T>>1.3$) were unsuccessful.

Further, even axisymmetric bodies operate in 3D flows during manoeuvring or motions across a current. Therefore consideration of some angles of attack (some jaws) becomes unavoidable during estimation of performances of the designed bodies. During motions at some angle of attack the boundary layer may separate from a part of the body upstream of the suction ring and this is the substantial issue.

The simplest response to the issue would be to reduce the speed during turns, but such a response would not be always accepted as a satisfactory one. For motions at small and moderate angles of attack, the passive control must be carried out for a given small angle of attack. Then, as already manifested in [9] for head forms of the more slender axisymmetric bodies, only the upper meridian section will be kept as a constant pressure streamline, whereas other sections will be in the zone of an accelerating flow. With this correction to the design concept, the flat bow surface area and the hull fullness coefficient will be, however, smaller.

Returning to motions of 3D bodies at very small angles of attack, let us recall another useful feature of 3D constant pressure surfaces related to boundary layers on them. The velocity components in the 3D boundary layers can be generally described as

$$u(y)=\cos\beta f(\eta)+[U_\delta-\cos\beta f(\delta)]\,\eta^2[3-2\eta],$$
$$w(y)=\sin\beta\{f(\eta)-f(\delta)\,\eta^2[3-2\eta]\} \quad (3)$$

An additional energy is necessary for generation of secondary flows associated with $w(y)$ and this necessity increases C_D. However, as known since the study [10] (indeed applicable to any kind of boundary layers), 3D boundary layers without secondary flows ($\beta=0$) can exist over surfaces, where streamlines of the inviscid flow coincide with the surface geodesic curves. As noted in the monograph [11], such coincidence is mathematically proven for the surfaces with the constant pressure in steady flows of ideal incompressible fluid (just like the surfaces designed here). So, mitigating the secondary flows, the suggested passive flow control additionally reduces the hull form resistance.

5. CONCLUSIONS

1. The presented study manifests the possibility to sharply improve the performance of very short hulls in the range of Reynolds numbers typical for Autonomous Underwater Vehicles by employing of the drag reduction technology combining a passive flow control with an active flow control. The passive control consists of inserting constant pressure surfaces in the middle of the body. The active control consists of suction applied to the area of high adverse pressure gradients.
2. The achieved drag reduction will be very significant for L/B rates from 1.25 to 2.5. For

more slender hulls, the effect of this drag reduction technology is smaller.

3. The sensitivity of the suggested drag reduction technology to the suction intensity (to the active flow control parameter) and to the range of Reynolds number is determined. It was found that excessive suction would give reduce positive effect and the effective range of the suggested active flow control is limited by $Re<10^7$.
4. The provided design examples relate mainly to the axisymmetric flows. The employed design tools were step by step validated with known experimental data for axisymmetric bodies.
5. An important methodical aspect is selection of CFD design tools. Design of surfaces with two constant pressure zones (as shown in Figures.3 and 6) requires rather a special computer code. Further, the maximum positive effect of suction occurs for situations where the suction area is located close to the laminar – turbulent transition area. Therefore, the worldwide popular commercial CFD codes for fully turbulent flows can be employed neither in such body design, nor in the design computational validation.

6. REFERENCES

1. HOERNER, S.F. *Fluid Dynamic Drag*, Authors Self Publication, NJ, 1965
2. BOURGOYNE, D.A., CECCIO, S.L., DOWLING, D.R. "Vortex shedding from a hydrofoil at high Reynolds number". *J. Fluid Mech*., v531, pp293–324, 2005
3. CASTILLO, L., WANG, X., GEORGE, W.K. "Separation Criterion for Turbulent Boundary Layers via Similarity Analysis", *ASME J. Fluids Eng.*, v126, pp297-304, 2004
4. AMROMIN, E.L. "Vehicles drag reduction with control of critical Reynolds number", *ASME J. Fluids Eng.*, v135, p101105, 2013
5. PATEL, V.C., NAKAYAMA, A, DAMIAN, R. "Measurement in the thick axissymmetric boundary layer near the tail of a body of revolution". *J. Fluid Mechanics*, v63, pp345-367, 1974
6. MICHEL, R. "Etude de la transition sur les profile d'aile: etablissement d'un critere de determination de point de transition et calcul de la traine de profile imcompressible, *ONERA Report 1/157A,* 1951
7. MEIER, H.U., KREPLIN, H.P. "Experimental Investigation of the Boundary Layer Transition and Separation on a body of revolution". *Zeitschrift for Flugwissenshaften and Weltraumforschung*, n2, pp65-70, 1980
8. ARNDT, R.E.A., AMROMIN, E.L., HAMBLETON, W. "Cavitation inception in the wake of a jet-driven body", *ASME J. Fluids Eng.*, v131, p111302, 2009
9. PASHIN, V.M., BUSHKOVSKII, V.A., AMROMIN, E.L. "Determination of Three-Dimensional Body Forms from Given Pressure Distribution over their Surfaces", *J. Ship Research*, v40, pp22-27, 1996
10. SEDNEY R. "Laminar boundary layer on a spinning cone at small angles of attack in a supersonic flow", *J. Aeronautic Sciences*, v24, pp430-456, 1957
11. BIRKHOFF, G. and ZARANTONELO, E. *Jets, Wakes and Cavities*. Ac. Press, 1957